



Retrospective Proposals for the Orbital Correction of GSAT0201 & GSAT0202

Sebastiano Buson¹ · Carlo Bettanini¹

Received: 27 October 2022 / Revised: 3 May 2023 / Accepted: 5 May 2023
© The Author(s) 2023

Abstract

On August 22, 2014, the first two Full Operational Capacity satellites of the Galileo constellation were launched from Kourou on a Soyuz ST-B rocket. Shortly after the insertion into the final orbit, the on-board telemetry showed the achieved orbit was different from the target highly inclined circular orbit, due to a failure in the Fregat upper stage attitude control system. This anomaly precluded nominal operations in the Galileo constellation, as well as introducing limitations in the use of several of on-board subsystems. A recovery campaign took place in the winter of 2014 to change the two satellites' trajectories, so to reduce the entity of operative constraints and provide better communication with the ground segment. With no dedicated orbital thruster available, attitude thrusters were used effectively to modify and enhance the orbit and recover from a multi-system failure, making reinsertion in a GNSS constellation possible. This work investigates, by means of a numerical model, the best combination and sequence of maneuvers that could have been implemented in the recovery campaign to satisfy most proposed drivers with the given Δv budget. The results show that different final orbits with the same resonance but lower eccentricity could have been achieved.

Keywords GNSS · Orbit recovery · Orbit correction

List of Symbols

a	Semimajor axis
α	Angle between plane versors
γ	Flight path angle
e	Eccentricity
Δ_i	Change in inclination
$\Delta\Omega$	Change in right asc. of the asc. node
$\Delta_{tf_{\min}}$	Max diff. target-failed orbits
Δ_{tc}	Difference target-corrected orbits
$\Delta_{fc_{\max}}$	Max diff. failed-corrected orbits
$\Delta\theta$	Difference in S/Cs true anomalies
i	Inclination
m	Fuel mass
M	Mean anomaly
μ	Standard terrestrial constant
ω	Argument of perigee
Ω	Right asc. of the asc. node
R_{Earth}	Earth radius
σ	Standard deviation of parameters

T	Orbital period
θ	True anomaly
u	Argument of latitude
v	Satellite velocity

1 Introduction

Galileo is a free and open-to-everybody Global Navigation Satellite System created by the European Union through the European Space Agency. Its main aim is to provide a high-precision positioning, navigation and timing system to users all around the globe.

Following the successful launches of the Galileo In Orbit Validation satellites, the two first Full Operational Capacity satellites, GSAT0201 and GSAT0202, were launched with a Soyuz ST-B rocket from the Kourou spaceport on August 22, 2014. The launch acronym was VS09.

Hours after launch, the probes' telemetry showed that the injection operations had failed, resulting in a final orbit which was degraded so much that the nominal operational trajectory could not be reached with any series of maneuvers. The interruption of flow to one of the upper stage hydrazine attitude

✉ Sebastiano Buson
sebastianobuson@gmail.com

¹ Department of Industrial Engineering, University of Padova,
via Venezia 1, Padua, Italy

Table 1 GSAT0201 on 22/08/14, 16:15:08 UTC

GSAT0201	Obs	Δ_{if}	$\Delta_{\text{if}}/\sigma$
a [km]	26197.6	-3715	111
e	0.232	0.23	698
i [deg]	49.77	-5.35	134
Ω [deg]	87.47	-13.19	330
ω [deg]	24.73	-	-
$u = \theta + \omega$ [deg]	249.04	7.79	/

Table 2 GSAT0202 on 22/08/14, 16:15:08 UTC

GSAT0202	Obs	Δ_{if}	$\Delta_{\text{if}}/\sigma$
a [km]	26181.3	-3706	111
e	0.233	0.23	698
i [deg]	49.77	-5.35	134
Ω [deg]	87.48	-13.19	330
ω [deg]	24.88	-	-
$u = \theta + \omega$ [deg]	249.76	7.78	/

thrusters meant that the attitude of VS09 payload at injection was 35.34° away from the right direction [1].

As a consequence of the failed circularization, the programmed schedule had to be abandoned, and the mission had to be totally redefined. The high eccentricity and short semimajor axis of the orbit were in fact detrimental for many attitude determination sensors, and, in general, the use of the satellites for Earth navigation purposes was compromised.

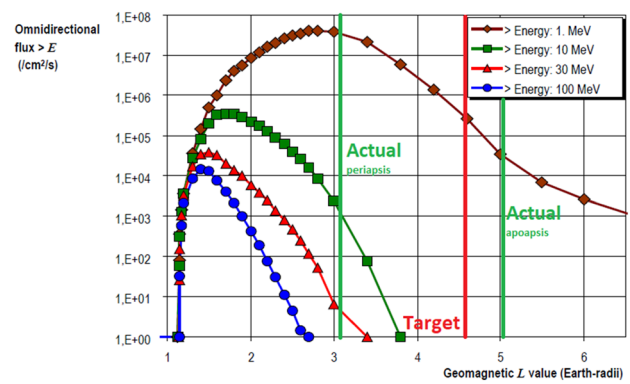
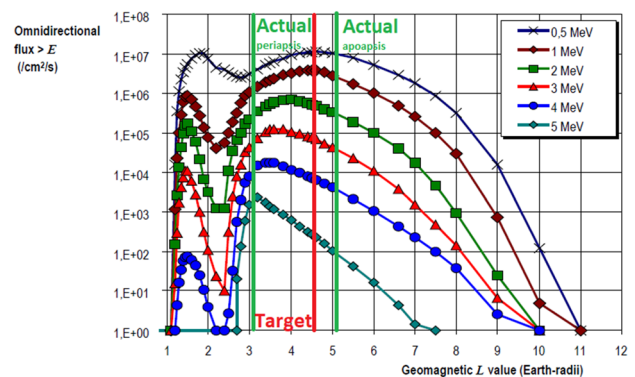
Tables 1 and 2 show the orbital parameters of the orbit resulting from the failed injection, as well as the differences with respect to the parameters of the injection target, both in absolute values and over the launch accuracy values [2].

The presence of attitude control thrusters on the spacecrafts entailed the possibility of mission recovery by means of an orbital correction. This situation was used as a benchmark problem to test a numerical orbit optimization method based on analytical orbital mechanics equations that, given a certain impulsive Δv budget, uses it to reach the combination of orbital parameters that best satisfy a set of recovery drivers.

The method is in accordance with what was found by Lawden [3] and by Plimmer [4] in regard of fuel optimization of impulsive transfers between two co-planar and co-axial orbits, and is useful to determine the exact entity of apsidal burns to reach a certain (a, e) .

2 Orbit Insertion Failure Limitations and Recovery Drivers

The failed injection exposed the spacecraft to many criticalities [6].

**Fig. 1** Protons omnidirectional flux as function of distance from Earth. Credits: [5]**Fig. 2** Electrons omnidirectional flux as function of distance from Earth. Credits: [5]

The altitude range, different from the planned MEO circular one, meant that the satellites were deep in the most energetic parts of the Van Allen belts. Galileo FOC spacecrafts are constructed in order to comply to the levels of radiation present at $\sim 4.6R_{\text{Earth}}$, that is a region where there are high fluxes of electrons with $< 5\text{MeV}$ energy levels. GSAT0201 and GSAT0202 instead oscillated between $\sim 3.1R_{\text{Earth}}$ and $\sim 5.1R_{\text{Earth}}$, see Figs. 1 and 2. This meant that the orbit crossed regions where the presence of high-energy protons is relevant, especially approaching lower altitudes.

The change in altitude entailed problems with Earth horizon sensors, which are operational only for heights above 15,331 km. This meant that for $\theta \in [-53^\circ, 53^\circ]$, that is for $\sim 18.8\%$ of the orbital period, Earth sensors could not be used.

Another attitude control subsystem that is deeply impacted by the different kind of orbit are gyroscopes. Since the avionics' On Orbit Propagation software corrects their angular momentum using simplified expressions which are valid for circular orbits only, they work correctly only for a narrow range of eccentricities. For the actual VS09 satellites

orbits, nadir-pointing can diverge up to $5^\circ/\text{h}$ when at perigee, for a total angular displacement of $\sim 12^\circ$ during the Earth sensors' blackout.

The change of orbit also has consequences in the communications between the satellite and the ground segment. In particular, the signal sent from the satellites suffers from a wider range of Doppler shift, and there is presence of lower-than-normal visibility window periods.

Moreover, the on-board MASER and rubidium clocks are affected by wider periodic variations on their clock rate due to an increased relativistic gravitational redshift.

2.1 Recovery Drivers

The initial objective for the probes launched on August 22, 2014 was the insertion into specific slots of the Galileo global navigation satellite system constellation. In presence of a multisystem failure and limited possibilities for orbit corrections, priorities change.

The recovery was possible thanks to the hydrazine thrusters of the attitude control system of the probes, which could ideally express a total of $\Delta v = 0.192 \text{ km/s}$.

The drivers should satisfy a hierarchy of requirements, which, listed from the most important to the least important, are (1) reducing the risk of collision with other objects in orbit, (2) reducing the damage to on-board functioning subsystems, (3) allow for the satellites to be able to operate, (4) insert the spacecrafts into the Galileo constellation.

Translated qualitatively, the drivers are the following:

- I. Reserve enough fuel for collision avoidance with other orbiting bodies and for attitude control.
- II. Reduce the harmful radiation dose on the spacecrafts and their degradation rate.
- III. Allow for baseline operations of all attitude and orbit control system sensors.
- IV. Reduce the operational burden on the satellites communications system.
- V. Insert the satellites into orbits with a certain ground track repeatability, similar to the one of the Galileo constellation.
- VI. Reduce secular drifts due to Earth oblateness.
- VII. Insert the probes into specific orbital planes.

The perfect scenario would consist in managing to shift the probes into their original target slots using the less fuel possible, which would guarantee that all priorities are satisfied.

Therefore maneuvers should aim to (1) increase of the semimajor axis a up to a specific value, (2) reduce the orbit eccentricity e as much as possible, (3) change i and Ω to fit into Galileo constellation planes.

Since the aim of the correction is a circular orbit, changes in ω are not contemplated. Assuming perfect timing, maneuvers should place the satellites so that $\Delta\theta \rightarrow 180^\circ$.

3 Assumptions on Simulation of Recovery Maneuvers

Impulsive maneuvers are defined as instantaneous changes of the velocity vector \mathbf{v} , both in magnitude and in direction. This simplification allows us to compute more easily the evolution of the state vector of an orbiting body, since the position vector \mathbf{r} is fixed under this hypothesis. Furthermore, this ensures the possibility to choose the specific points where performance is at its optimum.

Therefore, in the analysis that follows, maneuvers are going to be considered as impulsive.

In the two-body problem, the instantaneous speed change magnitude Δv between two velocity vectors \mathbf{v}_1 and \mathbf{v}_2 depends on the magnitude of the two vectors, on their flight path angles γ_1 and γ_2 and on the angle between their respective orbital planes versors α . To take place, the two orbits must have at least one point in common [7].

The equation that relates all these variables is the following:

$$\begin{cases} \Delta v = \sqrt{v_1^2 + v_2^2 - 2v_1v_2\Gamma} \\ \Gamma = \cos(\gamma_2 - \gamma_1) - \cos(\gamma_1)\cos(\gamma_2)[1 - \cos(\alpha)] \end{cases} \quad (1)$$

It is possible to see that, maintaining the velocity vectors' magnitudes constant, Δv is at its minimum when the cosine term Γ is at its maximum.

The cosine term Γ is limited to the interval $[-1, 1]$. Its maximum value can be reached when:

- Both flight path angles are equal to one another and assume the value of $\pm 90^\circ$, for any α . Yet, no elliptical orbit can reach such flight path angles since:

$$\begin{cases} \gamma(\theta) = \arctan\left(\frac{e \sin \theta}{1 + e \cos \theta}\right) \leq \gamma_{max} \\ \gamma_{max} = \arctan\left(\frac{e}{\sqrt{1 - e^2}}\right) < 90^\circ \end{cases} \quad (2)$$

- With $\alpha = 180^\circ$, one flight path angle is the opposite of the other. This means $\Delta \mathbf{v}$ inverts the direction of orbit;
- With $\alpha = 0^\circ$, both flight path angles remain equal. This means $\Delta \mathbf{v}$ cannot invert the direction of orbit;

All things considered, the most efficient operations for an elliptical orbit can be performed only if all velocity vectors \mathbf{v}_1 , \mathbf{v}_2 and $\Delta \mathbf{v}$ lie on the same direction.

3.1 Pure Plane Rotations Options

Before analysing the behaviour of the most efficient operations, pure plane rotations should be considered, so to see if any remarkable orbits for recovery can be found.

Rearranging Eq. 1, the formula can be solved to find the highest value of α . For pure plane rotations, where $\gamma_1 = \gamma_2$ and $v_1 = v_2$, α is equal to:

$$\alpha = 2 \arcsin \left(\frac{\Delta v}{2v_1 \cos(\gamma)} \right), \quad (3)$$

where $v_1 \cos(\gamma) = v_{\perp}$. Its minimum value, which allows us to find the maximum α , is found at apoapsis.

The relation of α with inclination i and RAAN Ω is the following:

$$\cos(\alpha) = \cos(\Delta\Omega) \sin(i_1) \sin(i_2) + \cos(i_1) \cdot \cos(i_2) \quad (4)$$

Equations 3 and 4 can be used to find the relation between Δi and $\Delta\Omega$ for the most efficient pure plane maneuver.

Applying these angular difference on our actual orbits, the results are still very far from nominality, considering the required accuracy, as it can be seen in Fig. 3. In Table 3, the maximum difference between failed and corrected orbit $\Delta i_{c_{max}}$ and the minimum difference between corrected and target values $\Delta i_{c_{min}}$ of i and Ω are reported.

As it can be seen, even when using all the fuel, nominality cannot be reached for the orbital plane parameters.

For this reason, any pure plane change maneuvers for the orbit recovery proposals are going to be ruled out, focusing only on in-plane maneuvers.

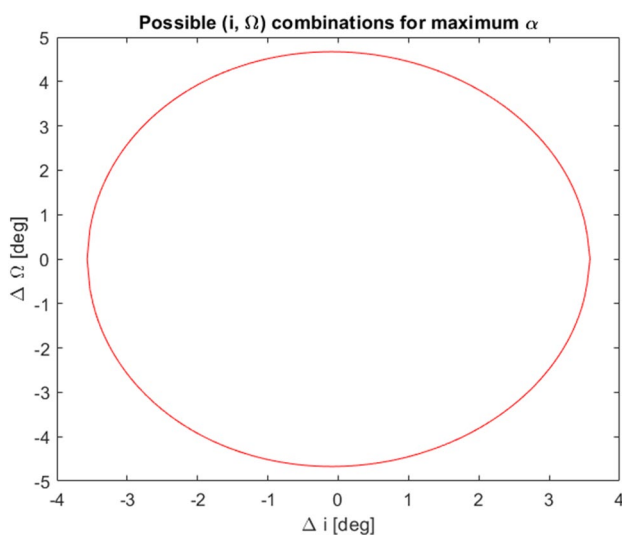


Fig. 3 Possible (i, Ω) combinations for apogee pure plane maneuvers, assuming $e = 0.233$, $a = 26200\text{km}$, $\Delta v = 0.192 \text{ km/s}$

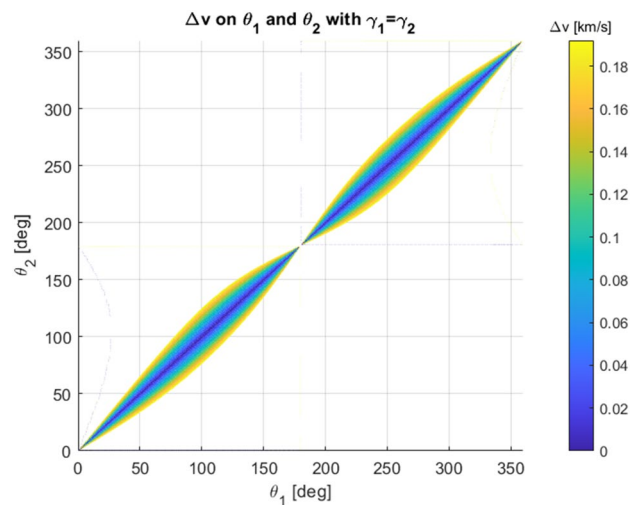


Fig. 4 Possible Δv values when $\gamma_1 = \gamma_2$, $e_1 = 0.233$ and $a_1 = 26,200 \text{ km}$

3.2 In-Plane Maneuvers

In this analysis, only the most efficient scenario will be considered, that is aligned velocity vectors. In general, the magnitude of the velocity vector $v(\theta)$ in any point of a keplerian orbit can be written as:

$$v = \sqrt{\frac{\mu(1 + e^2 + 2e \cos \theta)}{a(1 - e^2)}}. \quad (5)$$

Introducing Eq. 5 into Eq. 1 and imposing the following conditions:

- Same flight path angle:

$$\gamma_1 = \frac{e_1 \sin(\theta_1)}{1 + e_1 \cos(\theta_1)} = \frac{e_2 \sin(\theta_2)}{1 + e_2 \cos(\theta_2)} = \gamma_2 \quad (6)$$

- Same fixed position:

$$r_1 = \frac{a_1(1 - e_1^2)}{1 + e_1 \cos(\theta_1)} = \frac{a_2(1 - e_2^2)}{1 + e_2 \cos(\theta_2)} = r_2 \quad (7)$$

reduces the general Δv formula into the following set of equations, whose solutions can be seen in Fig. 4:

Table 3 Pure plane maneuvers performances

	Pure i corr	Pure Ω corr
$\Delta i_{c_{max}}$ [deg]	± 3.57	± 4.67
$\Delta i_{c_{min}}$ [deg]	2.66	8.51
$\Delta i_c / \sigma$	66.5	127.65

$$\begin{cases} \Delta v = \sqrt{\mu} \left(\sqrt{\frac{(1+e_2^2+2e_2 \cos \theta_2)}{a_2(1-e_2^2)}} - \sqrt{\frac{(1+e_1^2+2e_1 \cos \theta_1)}{a_1(1-e_1^2)}} \right) \\ e_2 = \frac{\tan(\gamma_1)}{\sin(\theta_2) - \cos(\theta_2) \tan(\gamma_1)} \\ a_2 = \frac{1+e_2 \cos(\theta_2)}{1+e_1 \cos(\theta_1)} \frac{1-e_1^2}{1-e_2^2} a_1 \end{cases} \quad (8)$$

$\implies \Delta v = f(\theta_1, \theta_2)$

Yet, such maneuvers would waste part of their performance into the rotation of the apsis line [7]:

$$\eta = \theta_2 - \theta_1 = f(\theta_1, \Delta v). \quad (9)$$

The only points where this rotation cannot happen is at the apses, that is when $\sin(\theta_1) = \sin(\theta_2) = 0$. In any other case, all the conditions can be satisfied only if there is no maneuver at all.

$$\begin{cases} \theta_1 = \theta_2 & \text{eq. (7)} \\ \sin(\theta_1) \neq 0 & \text{eq. (6)} \end{cases} \begin{cases} e_1 = e_2 \\ a_1 = a_2 \\ \Delta v = 0 \end{cases} \quad (10)$$

This means that the most efficient in-plane maneuvers which change only a and e can happen only at the periapsis or at the apoapsis.

3.2.1 Tangential Maneuvers at the Apsides

Note: equations of Sect. 3.2.1 are to be read in the following way:

- \pm : + for periapsis maneuvers, – for apoapsis ones;
- \pm : – for periapsis maneuvers, + for apoapsis ones.

In general, impulsive tangential maneuvers at the apses can be written as a linear combination of terms which depend only on a and e of the orbit's velocity. Assuming that the magnitude of Δv does not invert the eccentricity e , the general tangential impulsive maneuver equation is the following:

$$\Delta v_{\text{apsis}} = \sqrt{\frac{\mu}{a_{\text{fin}}}} \frac{1 \pm e_{\text{fin}}}{1 \mp e_{\text{fin}}} - \sqrt{\frac{\mu}{a_{\text{in}}}} \frac{1 \pm e_{\text{in}}}{1 \mp e_{\text{in}}}. \quad (11)$$

Since the burn position does not change during the impulse, the denominator in Eq. 11 is equal for both addenda. Thence, e and a of the resulting orbit will be equal to:

$$e_{\text{fin}} = \pm \left(\Delta v \sqrt{\frac{a_{\text{in}}(1 \mp e_{\text{in}})}{\mu}} + \sqrt{1 \pm e_{\text{in}}} \right) \mp 1 \quad (12)$$

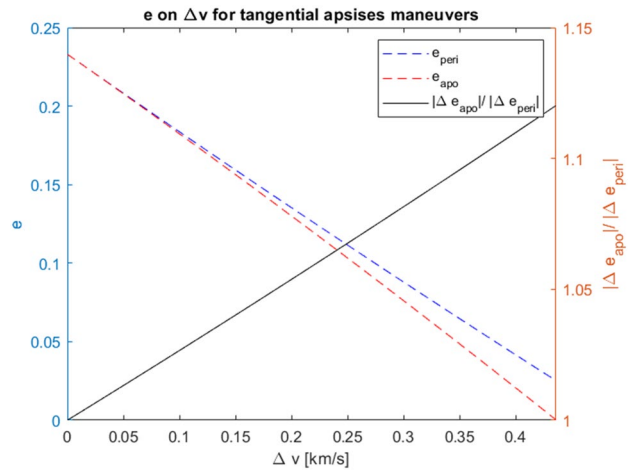


Fig. 5 Eccentricity on $|\Delta v|$ for tangential apses maneuvers ($e_1 = 0.233, a_1 = 26, 200$ km)

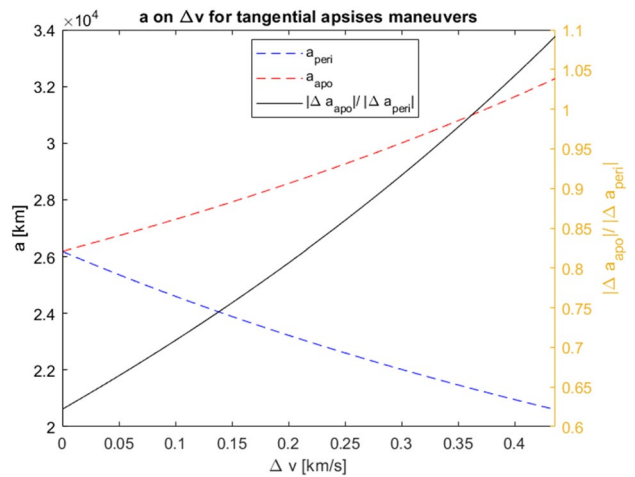


Fig. 6 Semimajor axis on $|\Delta v|$ for tangential apses maneuvers ($e_1 = 0.233, a_1 = 26, 200$ km)

$$a_{\text{fin}} = a_{\text{in}} \frac{1 \mp e_{\text{in}}}{1 \mp \left[\left(\Delta v \sqrt{\frac{a_{\text{in}}(1 \mp e_{\text{in}})}{\mu}} + \sqrt{1 \pm e_{\text{in}}} \right)^2 \mp 1 \right]}. \quad (13)$$

Supposing an attempt to reduce eccentricity, Δv must be positive at the apocenter, whereas it has to be negative at the pericenter.

Figures 5 and 6 show that, considering the problem's (a_1, e_1) :

- e decreases more if the same $|\Delta v|$ is applied at the apocenter;
- a increases for apocenter maneuvers and decreases for pericenter ones; yet, $|\Delta a|$ increases more if the same $|\Delta v|$ is applied at the perigee, for $\Delta v \in [0, \sim 0.35]$ km/s.

3.3 Δv Budget for the Correction

The maximum impulsive Δv the attitude control thrusters can express is 0.192 km/s for both satellites. Yet, some amount of propellant has to be reserved for the routine mission, for eventual safe modes, for collision avoidance and for station keeping.

Furthermore, there is the need to account for inefficiencies in the recovery operations, caused by the non-impulsiveness of real maneuvers and by possible errors in firing timing and duration.

For these reasons, real maneuvers can be approximated as ideal, both in timing and duration of the impulse, by reducing the total Δv which is used as in the orbital correction.

To conduct a meaningful comparison between the retrospective proposals and the actual recovery scenario, the same Δv budget ideal approximation the Galileo recovery team used will be utilized [8].

Therefore, $\Delta v = 0.16$ km/s for both spacecrafts.

4 Numerical Resolution of the Problem

4.1 Numerical Estimation of the Recovery Drivers

To elaborate the recovery orbits and the necessary maneuvers, a numerical estimation of the recovery drivers must be performed with respect to a and e .

- **Baseline operations of AOCS sensors:** the periapsis altitude must be higher than 15,331 km;
- **Communications burden reduction:** the orbit should have the lower e possible;
- **Ground track repeatability:** the ground track of the couple should repeat every 10 days. Every satellite will have to complete a finite amount of revolutions every 20

days. The orbital period has to be close to the nominal Galileo one;

- **Reduction J2 drifts, radiation:** a should be raised.

Quantitatively:

$$\begin{cases} a(1 - e) > 21,704 \text{ km} & \text{AOCS sensors} \\ e \rightarrow 0 & \text{Communications} \\ \sqrt{\frac{4\pi^2}{\mu} a^3} \begin{cases} \rightarrow \frac{10}{d} \\ = \frac{20}{n}d, n \in \mathbb{N} \end{cases} & \text{Resonance} \\ a \rightarrow \infty & \text{J2 drifts, radiation} \end{cases} \quad (14)$$

The most stringent constraint is the one on the ground track repeatability. In fact, there is only one couple of maneuvers with the first burn at apogee that can inject a body into an orbit with a certain combination of (a, e) for a given total Δv .

4.2 Numerical Model for the Optimization

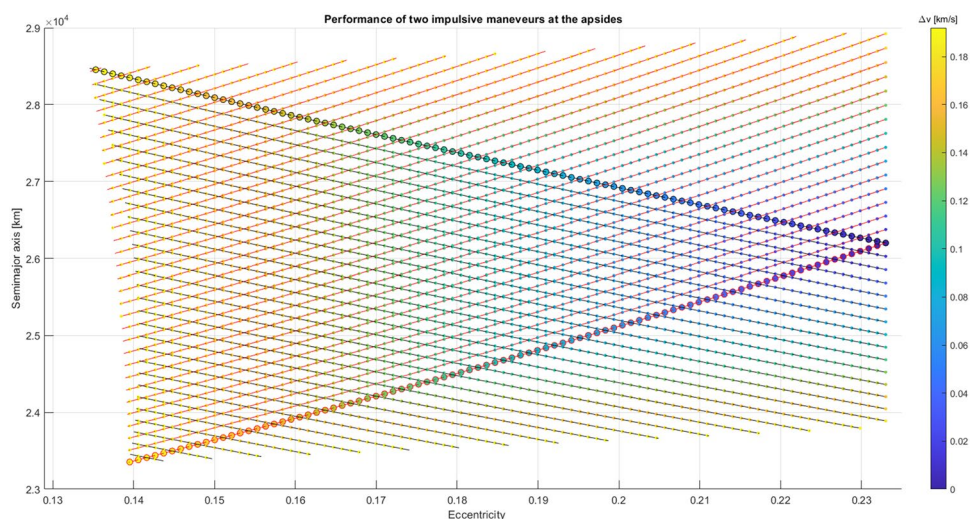
The numerical optimization model developed aims for the resolution of the series of two apsidal impulsive maneuvers alternatively performed problem. It implements Eqs. 12 and 13 and solves them different values of Δv s of two apsidal maneuvers, returning as outputs the semimajor axis and the eccentricity of the final orbit. Moreover, it calculates both the two masses of propellant used during both maneuvers and the remaining fuel mass.

Figure 7 is a visual representation of the model a and e outputs for different values of $\Delta v_{\text{tot}} = \Delta v_{\text{apo}} + \Delta v_{\text{peri}}$.

The most remarkable aspect of it is that, given a certain $(a_{\text{fin}}, \Delta v_{\text{tot}})$, if the first maneuver is performed at apogee, the final eccentricity e_{fin} will be lower than if it were performed at perigee. Moreover, the smallest value of e_{fin} is reached for a single maneuver at apogee.

From this analysis on impulsive maneuvers, it was found out that the best way to achieve the most recovery objectives

Fig. 7 Performance of two apsidal impulsive maneuvers



is by performing a combination of two tangential maneuvers, the former and main burn at apogee in the direction of orbit and the latter, a fine positioning maneuver in the opposite sense of orbit, at perigee.

This finding, together with the total Δv budget and the numerical estimation of recovery drivers, allows for the computation of maneuver and orbital parameters of the optimized solutions.

4.3 Proposed Recovery Orbits and Maneuver Sequence

Some relevant data can be extrapolated from the numerical model. Table 4 reports the orbital parameters and maneuvers-associated values of the proposed recovery orbits obtained by numerical iterations. For each orbital period, its associated semimajor axis is shown. The lowest eccentricity obtainable for each a with $\Delta v_{\text{tot}} = 0.16 \text{ km/s}$ is also shown, as well as the repartition of fuel burnt at apogee and perigee, both in terms of Δv and mass.

It is possible to notice the slight differences in the actual orbits parameters ($a_{0202} - a_{0201} = -16.3 \text{ km}$, $e_{0202} - e_{0201} = 0.001$) are perpetuated in the final recovery orbits. In fact, the eccentricity for the same target a and the same given Δv is different by about a part in a thousand.

Fuel mass: the remaining fuel mass m_{rem} decreases slightly for decreasing semimajor axes, as the necessary propellant mass for the perigee maneuver m_{peri} increases to ensure the minimum eccentricity possible. The maximum remaining fuel mass would allow for an impulsive maneuver of $\Delta v = 0.031 \text{ km/s}$.

Exposure to Van Allen belts: the harmful proton radiation dose decreases for every single orbit with respect to the actual trajectories, since the periapsis passes from being $r_{\text{peri}} \sim 3.1 R_{\text{Earth}}$ to being in the range $r_{\text{peri}} \in [3.48, 3.73] R_{\text{Earth}}$. The reduction of proton omnidirectional flux for the 37/20 orbits at perigee is about one order of magnitude.

Periapsis altitude: furthermore, the altitude at periapsis is over the baseline operation lower AOCs limit of 15, 331 km for every proposal. The lowest periapsis is for GSAT0202 40/20 orbit with $r_{\text{peri}} = 16, 163.27 \text{ km}$, that is 832 km over the lower Earth sensors boundary.

Final eccentricity: even though the circularisation of the orbits is not possible, the final eccentricity of the two satellites can be lowered to $e \sim 0.15$ for all the proposals, that is to $\sim 64\%$ of the initial eccentricities. Therefore, the burden on the communications system can be reduced.

Secular angular variations: secular drifts of Ω , ω and M have a lower magnitude for higher semimajor axes, see Table 5.

In Table 6 orbits are ranked from first to last for each numerical requirement, according to how they fulfill them. Qualitative requirements do not have ranking.

It is possible to see that the best orbit attainable is the one with an orbital period of 20/37d.

Since the spacecrafts must be injected in the same trajectory, the final eccentricity cannot be different between the two probes. Therefore, both will be fired in GSAT0202's 20/37 (a, e) (see Table 7).

Time sequence between corrections: the timing of maneuver is crucial in orbital correction. The difference between the failed orbits' Ω and ω can be decreased by correcting the satellites in two different moment of time, thanks to different rates of secular variation of the two parameters for orbits with different (a, e). It's also essential to place the satellites in such a way that $\Delta\theta$ becomes as close to 180 degrees as possible. By executing corrections for GSAT0201 and GSAT0202 at specific moments, these objectives can be partially accomplished without utilizing any fuel.

The difference in true and mean anomaly changes over time between the two satellites, due to the different mean motion and to secular perturbations when in different orbits.

From Fig. 8 it can be seen that $\Delta\theta \simeq 180^\circ$ is reached in a period that goes from 68 days to 98 days from the reference epoch of Table 2, independently from which satellite is corrected first.

Following the timetable for orbit correction of Table 8, $\Delta\theta$ oscillates between 170° and 184° , as it can be seen in Fig. 9. The oscillations are due to the different angular velocities that elliptic orbits possess for different true anomalies.

Moreover, in this lapse of time, Ω and ω vary. Table 9 details the time dependent orbital parameters.

Table 4 Proposals for the orbit recovery of GSAT0201 and GSAT0202

T [d]	a [km]	e	Δv_{apo} [km/s]	Δv_{peri} [km/s]	m_{apo} [kg]	m_{peri} [kg]	m_{rem} [kg]
20/37	27978.7	0.15015	0.1572	-0.0027	56.27	1.03	10.70
20/38	27485.7	0.15019	0.1406	-0.0194	50.51	7.17	10.32
20/39	27013.8	0.15036	0.1252	-0.0358	45.14	12.82	10.04
20/40	26561.7	0.15053	0.1081	-0.0519	39.17	18.98	9.85
20/37	27978.7	0.15119	0.1578	-0.0022	56.50	0.78	10.72
20/38	27485.7	0.15124	0.1412	-0.0188	50.74	6.92	10.34
20/39	27013.8	0.15136	0.1249	-0.0351	45.04	12.92	10.04
20/40	26561.7	0.15155	0.1088	-0.0512	39.40	18.75	9.85

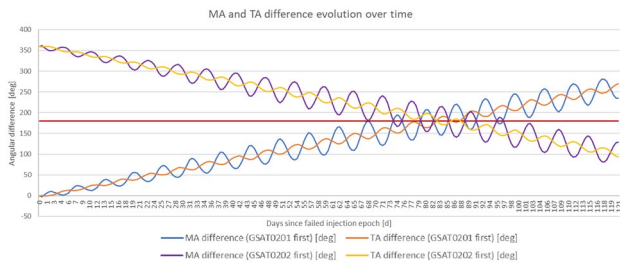


Fig. 8 Mean and true anomaly difference evolution between the two corrections

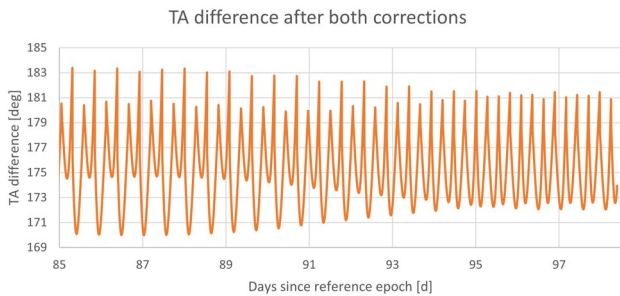


Fig. 9 True anomaly difference evolution after corrections

Table 5 Secular angular variation every 20 days, for $e \approx 0.15$

	$\Delta\Omega$ [deg]	$\Delta\omega$ [deg]	ΔM [deg]
37/20	-0.76	0.64	0.15
38/20	-0.81	0.68	0.16
39/20	-0.86	0.72	0.17
40/20	-0.91	0.77	0.18

Table 6 Satisfaction of Sect. 2.1 recovery drivers

	I	II	III	IV	V	VI	VII
20/37	1st	1st	✓	1st	✓	1st	×
20/38	2nd	2nd	✓	2nd	✓	2nd	×
20/39	3rd	3rd	✓	3rd	✓	3rd	×
20/40	4th	4th	✓	4th	✓	4th	×

5 Comparison Between Retrospective Proposal and Real Orbits

5.1 Real Recovery Operations

Operations to correct the orbit of GSAT0201 and GSAT0202 began with the handover of the satellites monitoring from the LEOP center to the Galileo Center on 26/09/14, 12:00:00 UTC [10].

Table 7 Time independent orbital parameters and maneuvers data for the corrected orbit

	GSAT0201	GSAT0202
a [km]	27,978.7	27,978.7
e	0.15119	0.15119
i [deg]	49.77	49.77
Δv_{apo} [km/s]	0.1561	0.1578
Δv_{peri} [km/s]	-0.0019	-0.0022
m_{rem} [kg]	11.41	10.72

Table 8 Timetable for correction

MJ2000 starting epoch t_0	26892.177
GSAT0202 apo. man	$t_0 + 0.399$ d
GSAT0202 peri. man	$t_0 + 0.668$ d
GSAT0201 apo. man	$t_0 + 84.239$ d
GSAT0201 peri. man	$t_0 + 84.504$ d

Table 9 Time dependent orbital parameters on 15/11/14, 04:27:12 UTC for the corrected orbit

	GSAT0201	GSAT0202
Ω [deg]	83.21	84.31
ω [deg]	28.31	27.54
$u = \theta + \omega$ [deg]	210.31	27.54

The Galileo team aimed for the reduction of operational burden on the AOCS system, the reduction of the exposure to the Van Allen belts radiation, the reduction of the eccentricity and an overall improvement of the Galileo constellation performance, that is aiming for the two satellites not to be visible together from any ground station at any time.

These recovery drivers had to be reached with a $\Delta v_{\text{tot}} = 0.16 \text{ km/s}$.

The final orbit the Galileo team aimed for was a resonant one, performing 37 orbits in 20 days, with the lowest eccentricity achievable. No variation in the angulation of the orbital plane was contemplated.

The correction was performed at first on GSAT0201, and consisted of nine apogee maneuvers and one perigee burn performed over the span of 14 days, from 5/11/14 to 19/11/14.

On the other hand, GSAT0202 underwent ten apoapsis maneuvers and one periapsis burn in a period of 39 days, from 22/1/15 to 2/3/15.

GSAT0201 and GSAT0202 both made their way into the Galileo constellation, since both were allowed to transmit their navigation message worldwide, respectively on 19/12/14 and on 25/3/15.

Table 10 Real and proposed satellites position on 5/3/15, 10:36:11 UTC. Credits: [9]

	a [km]	e	i [deg]	Ω [deg]	ω [deg]	$u = \theta + \omega$ [deg]
GSAT020—proposed	27,978.7	0.15119	49.77	79.01	31.84	55.11
GSAT0202—proposed	27,978.7	0.15119	49.77	80.10	31.07	224.99
GSAT0201—real	27,979.0	0.15600	49.78	78.74	32.24	212.65
GSAT0202—real	27,978.5	0.15600	49.88	77.52	34.35	34.35

5.2 Comparison with Retrospective Proposal

The orbit that the Galileo team aimed for has the same resonance as the one found in this analysis, that is the 20/37 orbit. In Table 10 the orbital parameters of proposed and real orbits are reported. In general, the proposed orbits have a lower eccentricity than the real correction trajectories. The relative difference between the two scenarios amounts to 3.083% the real eccentricity.

Moreover, the number of burns in the real scenario was higher than just two, since non-impulsive maneuvers are more efficient if the burn time tends to instantaneity. Yet, since recovery operations cannot go on for a long period of time, the number of maneuvers still has to be low and finite.

6 Conclusions

The failure in the injection procedures of the payload in flight VS09 left the two first FOC Galileo satellites in non-nominal orbits which were completely out of range from a complete recovery using their own propulsion system and were not usable for navigation purposes, due to problems at different subsystems.

After the recovery of failed non-orbit dependant subsystems on both probes, an improvement of the trajectory was possible. This could enable the probes to use their GNSS payload, and as a result the two satellites have been broadcasting from 05/08/2016 to 18/02/2021 [11].

After having considered all the possible maneuvers for the correction, a numerical model for the repartition of Δv over two apsidal maneuvers was developed, which allowed for the calculation of the maneuvers Δv to reach the orbits that best satisfy most of the drivers we elaborated. The Δv budget constraint that was set accounted for the necessary reserve fuel, for inefficiencies due to deviation of real maneuvers from instantaneity and for misfirings both in orbital timing and total duration.

Using the method on this problem, it can be concluded that best trajectories have a resonance of 37 orbits every 20 days, close to the nominal one of 34 orbits every 20 days. The timing of the maneuvers was also considered, to allow for the quasi-alterability of the satellites every 10 days.

The final orbits are consistent with the Galileo team's, with a slight improvement on the final eccentricity, which is lower by 3.083%.

Funding Open access funding provided by Università degli Studi di Padova within the CRUI-CARE Agreement.

Data availability No additional data to be shared.

Declarations

Conflict of Interest On behalf of all the authors, the corresponding author states that there is no conflict of interest.

Open Access This article is licensed under a Creative Commons Attribution 4.0 International License, which permits use, sharing, adaptation, distribution and reproduction in any medium or format, as long as you give appropriate credit to the original author(s) and the source, provide a link to the Creative Commons licence, and indicate if changes were made. The images or other third party material in this article are included in the article's Creative Commons licence, unless indicated otherwise in a credit line to the material. If material is not included in the article's Creative Commons licence and your intended use is not permitted by statutory regulation or exceeds the permitted use, you will need to obtain permission directly from the copyright holder. To view a copy of this licence, visit <http://creativecommons.org/licenses/by/4.0/>.

References

1. Ariespace. Vol VS09—Résultats de la Commission d'Enquête Indépendante relatifs à l'anomalie survenue sur l'étage supérieur Fregat du lanceur Soyuz. (2014)
2. Ariespace. Soyuz at the Guiana Space Centre—user's manual. <https://www.arianespace.com/wp-content/uploads/2015/09/Soyuz-Users-Manual-March-2012.pdf> (2012). Accessed 25 Jul 2022
3. Lawden, D.F.: Impulsive transfer between elliptical orbits. In: Leitmann, G. (ed.) Optimization Techniques. Mathematics in Science and Engineering, vol. 5, pp. 323–351. Elsevier (1962)
4. R. N. A. Plimmer. Fuel Requirements for Inter-Orbital Transfer of a Rocket. In: Xth International Astronautical Congress London 1959 / X. Internationaler Astronautischer Kongress / Xe Congrès International d'Astronautique. Ed. by Friedrich Hecht. Berlin, Heidelberg: Springer Berlin Heidelberg, 1960, pp. 911–932
5. Kivelson, M.G.: Introduction to Space Physics. Cambridge University Press, Berlin (1995). <https://doi.org/10.1017/9781139878296>
6. Côme, H., et al.: GALILEO 5 and 6 LEOP or how to handle and recover two of the most feared failures occurring simultaneously. <https://doi.org/10.2514/6.2016-2506> (2016)

7. Curtis, H.D.: *Orbital Mechanics for Engineering Students*, 4th edn. Elsevier Aerospace Engineering Series (2020)
8. Navarro-Reyes, D., et al.: Galileo first FOC launch: recovery mission design. In: *Proceedings of the 25th International Symposium on Space Flight Dynamics ISSFD, Munich, Germany (2015)*
9. Carlier, N., et al.: Spacecraft recovery operations conducted to the Galileo FOC-1 L3. In: *Proceedings of the 25th International Symposium on Space Flight Dynamics ISSFD, Munich, Germany (2015)*
10. Ayala, A., et al.: Galileo extended slots characterisation and relation with the nominal constellation. (2016)
11. Notice advisory to Galileo users (NAGU) 2021008. <https://www.gsc-europa.eu/notice-advisory-to-galileo-users-nagu-2021008>. Accessed 27 Mar 2023

Publisher's Note Springer Nature remains neutral with regard to jurisdictional claims in published maps and institutional affiliations.